

NEW INSIGHTS ON NITROGEN DOPING*

D. Bafia[†], A. Grassellino, A. Romanenko, M. Checchin, O. S. Melnychuk, D. A. Sergatskov,
 Fermi National Accelerator Laboratory, Batavia, USA
 J. F. Zasadzinski, ¹Illinois Institute of Technology, Chicago, USA

Abstract

This paper covers a systematic study of the quench in nitrogen doped cavities: a cavity was sequentially treated/reset with different N-doping recipes which are known to produce different levels of quench field. Analysis of cavity heating profiles using TMAP are used to gain insight on the origins of quench; new recipes demonstrate the possibility to increase quench fields well beyond 30 MV/m. In addition, a new signature of nitrogen doping is explored, namely, a dip in the superconducting resonant frequency below the normal conducting value just below the critical transition temperature, giving further insights on the mechanisms responsible for the large increase in performance of cavities subject to this surface treatment.

INTRODUCTION

The 2/6 nitrogen doping surface treatment of Nb superconducting radio-frequency (SRF) resonators has been shown to produce cavities with very high quality factors [1, 2]. However, the quench field of cavities subject to this treatment are lower than are achieved via others [3-6]. The simultaneous improvement of the quality factor and the accelerating gradient of N-doped cavities is necessary to decrease the cost of future accelerators.

To gain insight on the current limitations of quench in 2/6 N-doped cavities, the performance of a 1.3 GHz single cell SRF cavity subject to sequential treatments to the optimized variants of N-doping shown in Table 1, which have been shown to give accelerating gradients well above 30 MV/m [7], are investigated via RF testing and the thermometry mapping set up described in [8]. Heating profiles of the cavity post sequential treatments are used to draw conclusions on the location and possible nature of quench in N-doped cavities.

In addition to insights on quench mechanisms, a systematic study of a newly observed signature of nitrogen doped cavities is discussed and presented, namely, the prominent dip in the superconducting (SCing) resonant frequency below the normal conducting (NCing) value that exists just below the critical transition temperature. The effects of nitrogen concentration and cavity design frequency on this dip are studied. A discussion of the origin of this dip is presented along with possible implications on the superconducting properties of the resonator. This dip in the resonant frequency could help in understanding the possible microscopic mechanisms responsible of the large increase in Q_0 of cavities subject to this surface treatment.

* This work was supported by the United States Department of Energy, Offices of High Energy Physics and Basic Energy Sciences under Contracts No. DE-AC05-06OR23177.

[†] dbafia@fnal.gov

Table 1: Optimized N-doping Treatment

2/6 Doping-Baseline	2/0 Doping-FNAL	3/60 Doping-JLab
800 C 3 h in UHV	800 C 3 h in UHV	800 C 3 h in UHV
800 C 2 min 25 mTorr N	800 C 2 min 25 mTorr N	800 C 3 min 25 mTorr N
800 C 6 min UHV	N/A	800 C 60 min UHV
5 μ m EP	5 μ m EP	5 μ m EP

QUENCH MECHANISMS IN N-DOPING

Sequential Study of Single Cell

The performance of the 1.3 GHz single cell cavity, AES025, post the sequential treatment to the recipes outlined in Table 1 with a 40 μ m EP reset of the surface in between is shown in Figure 1.

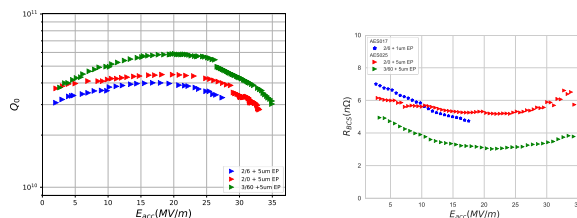


Figure 1: (Left) Q_0 vs E_{acc} measurements of AES025 post sequential treatments to the recipes outlined in Table 1. (Right) BCS resistance vs E_{acc} of AES025 post sequential treatments. The curve for AES017 shown in blue is present due to the absence of low temperature data of AES025 post 2/6 N-doping.

Cavity AES025 post 2/6 N-doping gave a quench field of 27.5 MV/m with a max Q_0 of $4E10$. After resetting the cavity surface and treating with 2/0 doping, the quench field increased by about 6 MV/m, giving a final quench field of 33 MV/m and a max Q_0 of about $4.4E10$. Performing another RF surface reset and treating with 3/60 doping gave a quench field of an unprecedented value of 35 MV/m and max Q_0 of $5.9E10$. Note that the sudden drop in Q_0 at high gradients post 2/0 and 3/60 N-doping occurred after soft quench and is attributed to trapped flux. Processing increased the gradients to their final values. The BCS surface resistance for the cavity post 2/0 nitrogen doping is like that of a standard 2/6 nitrogen doped cavity. However, 3/60

Content from this work may be used under the terms of the CC BY 3.0 licence (© 2019). Any distribution of this work must maintain attribution to the author(s), title of the work, publisher, and DOI.

doping gives a very low BCS resistance, achieving a minimum of 3.5 nΩ at 21 MV/m.

Sequential TMAP Studies

The heating profiles of cavity AES025 post sequential optimized N-doping treatments is now presented. The 3/60 N-doping plus 10 μm EP treatment is first shown. The resulting Q₀ vs E_{acc} curve and TMAP profile taken just before quench are shown in Figure 2.

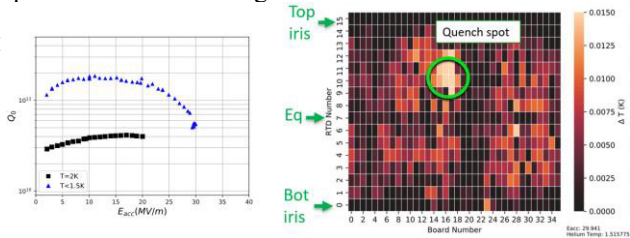


Figure 2: (Left) Q₀ vs E_{acc} curve of AES025 post 3/60+10 μm EP N-doping. (Right) TMAP profile taken just before quench with a helium bath temperature of ~1.5 K. Note that data was only taken up to 20 MV/m for T = 2 K to avoid quench.

The cavity quenched at 30 MV/m. Inspection of the heating profile just before quench shows that the quench spot was above the equator but there was uniform heating over the surface

After a 40 μm EP reset of surface, AES025 was subject to the 2/0+5 μm EP recipe. The RF and TMAP test results are shown in Figure 3. The cavity quenched at 18 MV/m, which is far earlier than was obtained for the first time this cavity received this same surface treatment, as shown in Figure 1. Further investigation of the furnace RGA scans showed that there were higher levels of impurities because the furnace had not been baked out for several months. As such, this nitrogen doping treatment is labelled as a failed 2/0 N-doping treatment; however, lessons may still be learned from the TMAP profile

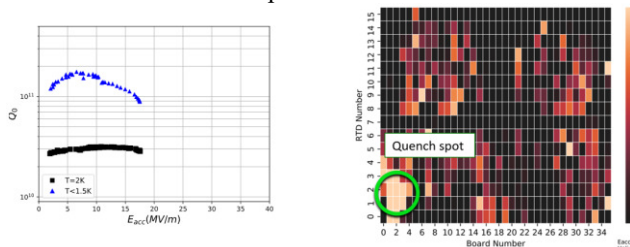


Figure 3: (Left) Q₀ vs E_{acc} curve of AES025 post of the failed N-doping treatment of 2/0+5 μm EP. (Right) TMAP profile taken just before quench with a helium bath temperature of ~1.5 K.

The heating profile shown in Figure 3 shows that there was very strong local heating near the bottom iris. The quench spot was located at the point of strongest pre-heating.

The surface of AES025 was again reset with another 40 μm EP and treated to a successful 2/0+5 μm EP nitrogen doping run. The testing results are displayed in Figure 4. This time, the cavity quenched at the extraordinarily high accelerating gradient of 38 MV/m at T < 1.5 K. The quench

spot of the cavity was just above the cavity equator. It is interesting to see that the point of strongest local pre-heating just before quench does not correspond to the quench spot.

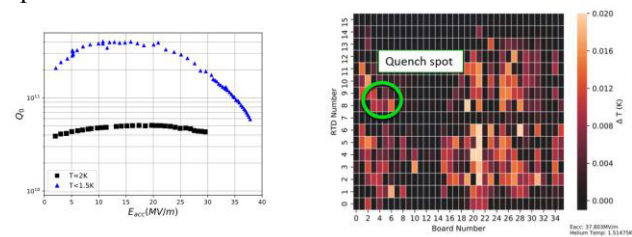


Figure 4: (Left) Q₀ vs E_{acc} curve of AES025 post 2/0+5 μm EP N-doping. (Right) TMAP profile taken just before quench with a helium bath temperature of ~1.5 K. Note that data was taken up to 30 MV/m for T = 2 K.

For the final test, AES025 received an additional 2 μm of EP, resulting in a doping treatment of 2/0+7 μm EP. The results are displayed in Figure 5. The additional 2 μm of EP appears to have drastically lowered the effect of nitrogen doping; the anti-Q slope has been replaced with the high field Q-slope (HFQS). Note, however, that the onset of the HFQS is about 10 MV/m higher than for standard EP cavities, which occurs at ~25 MV/m. The TMAP profile taken just before quench shows that the cavity quenched below the equator. As the cavity quenches at higher accelerating gradients, the location of quench tends to be closer to the equator.

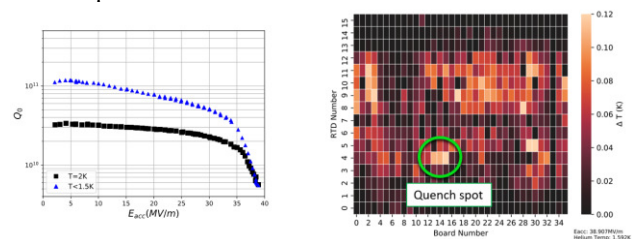


Figure 5: (Left) Q₀ vs E_{acc} curve of AES025 post 2/0+7 μm EP. (Right) TMAP profile taken just before quench with a helium bath temperature of ~1.5 K.

To gain more insight on the mechanisms responsible for the above quenches, the heating profiles as a function of the magnetic field of the RTD sensor located closest to the positions of quench for each respective test are shown in Figure 6. Both the 3/60+10 μm EP and successful 2/0+5 μm EP N-doping treatments show very little pre-heating before quench, with the highest temperature measured below 0.01K. Due to this lack of pre-heating, the quench mechanism of these tests is likely to be of magnetic origin. The quench location of the failed 2/0+5 μm EP N-doping, however, shows much stronger pre-heating, which starts at ~8 mT. The heating increases with the peak magnetic field until 40 mT, where a discrete jump occurs in the heating up to higher values. After this jump, the temperature continues to increase with field, reaching a value of ~1 K before quench. This jumping behavior was witnessed at the same field when then He bath was at a temperature of 2 K. This

discrete jump coupled with the strong heating might be indicative of the fact that the quench is due to the heating of a nitride that exists on the surface.

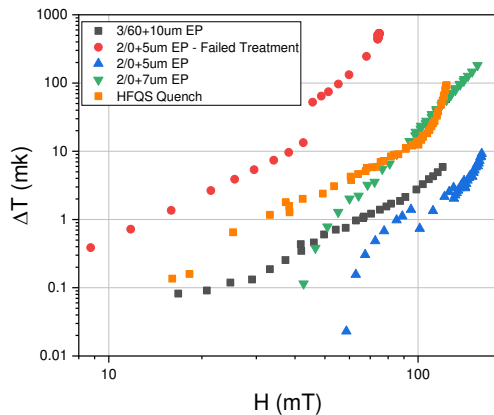


Figure 6: A log vs log plot of the measured temperature difference as a function of the peak magnetic field of the RTD located closest to the position of quench for each of the above TMAP studies. The He bath temperature was ~ 1.5 K. The heating profile of a cavity with high field Q-slope (HFQS) is shown in orange squares for comparison.

The last temperature profile studied is that of AES025 post 2/0+7 μm EP N-doping. The heating increases quickly with the peak magnetic field, reaching 0.2 K just before quench. As such, the quench might be of thermo-magnetic origins. The Q_0 vs E_{acc} curve of this last test post 2/0+7 μm EP N-doping showed the onset of HFQS. It is interesting to compare this heating profile with that of a cavity with strong HFQS. From Figure 6, it is seen that the heating profile of a cavity that experienced HFQS has a slope that is not as steep as the one observed in the 2/0+7 μm EP N-doping case. However, there is a sharp increase in the slope at 100 mT. This behavior is not observed in the 2/0+7 μm EP surface treatment even though HFQS is present.

To summarize, the quench of nitrogen doped cavities seems to be of either magnetic or thermo-magnetic origin. Higher (lower) quench fields of nitrogen doped cavities tend to have quench locations that are closer to the equator (iris). With some insights on the quench mechanisms of nitrogen doped Nb cavities obtained, attention is now turned to another feature of nitrogen doping; a prominent dip in the superconducting resonant frequency of the cavity below the normal conducting value that occurs just below the critical transition temperature. This is explored to gain possible insights on the mechanisms responsible for the large increase in quality factor of cavities subject to this surface treatment.

NEWLY DISCOVERED SIGNATURE OF N-DOPING: A DIP IN F_0 BELOW T_c

To explore the prominent dip in the superconducting resonant frequency below the normal conducting value that occurs just below the T_c of nitrogen doped Nb SRF

cavities, general features observed in frequency vs temperature (FvsT) data must first be discussed, as is done in the following section.

Zoology of FvsT Features

The resonant frequency of a cavity is measured at low fields with a network analyser as the cavity is warmed up through transition. The temperature is measured using Cernox RTD temperature sensors. As the cavity temperature increases, the resonant frequency of the cavity decreases due to the temperature dependence of the penetration depth, which increases with temperature. This is well described by the Gorter-Casimir two-fluid equation

$$\lambda(T) = \frac{\lambda_0}{\sqrt{1 - \left(\frac{T}{T_c}\right)^4}}, \quad (1)$$

where λ_0 is the penetration depth at zero Kelvin. However, deviations from this equation have been observed in experimental data as it does not consider the effect of the superconducting gap [9]. It is understood that any model that considers a gap will show that the penetration depth will more rapidly approach its zero-temperature value than one that does not [10]. As such, the superconducting gap of a resonator will influence its penetration depth into the surface, which in turn varies the profile of the resonant frequency as a function of temperature. The model states that as the temperature approaches T_c , the penetration depth goes to infinity, causing a discontinuity from the normal conducting value, which is governed by the normal conducting skin depth. Experimental data of Nb SRF cavities shows that the resonant frequency of a cavity remains finite in this region. Not only is the frequency finite, cavities also display five unique and distinct features in this region. Figure 7 outlines the five unique features observed in FNAL FvsT data.

The first feature is a lack thereof, in which there is a sharp transition from the superconducting (SCing) to the normal conducting (NCing) frequency, arbitrarily labelled ‘‘Standard’’. The second feature is described as a foot, which has a small hump before going NCing. The third feature is a dip with a bump, indicating that the frequency goes slightly below the NCing value and then back above it, after which it decreases back to the NCing value. The fourth feature is quite similar and only has a small bump. Lastly, there is a prominent dip in the SCing frequency below the NCing value. An explanation for the origins of this dip will be discussed later. Although all five features are fundamentally interesting, this prominent dip in the frequency is the most striking. As such, a systematic investigation of this dip will now be discussed.

Signature of N Doping

To investigate when this dip in the resonant frequency below the normal conducting value occurs, a single cell 1.3 GHz TESLA shaped Nb SRF cavity was subject to the

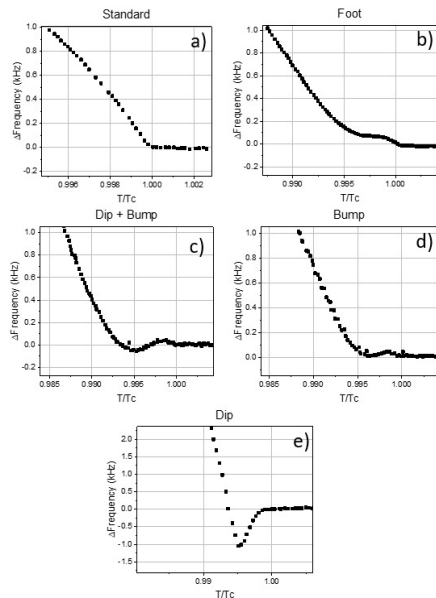


Figure 7: The five features observed in FNAL FvsT data. The normal conducting frequency is set to correspond to 0 Hz for each case.

following surface treatments with a surface reset of 40 μm via EP in between to compare same surface morphology; 75/120 C bake [4, 5], nitrogen infusion [3], and nitrogen doping. The cavity resonant frequency was then measured with a network analyser as the cavity was warmed up through transition. The results are outlined in Figure 8. Note that each curve is corrected for pressure differences within the dewar. Although the inset on the lower left of Figure 8 shows the expected differences in temperature dependence of the frequency due to differences in impurity structures, it is striking to see that the three surface treatments produce three of the five observed features near T_c discussed in Figure 7. This signifies that the surface preparation is responsible for these different features. The cavity post 75/120 C bake shows a foot near T_c . Nitrogen infusion, instead, gives a small dip with a bump. The cavity post nitrogen doping gives a prominent dip in the frequency vs temperature data just below T_c . For all the data studied (48 sets), this prominent dip occurs 100 % of the time in nitrogen doped cavities and appears to be a signature of it. Using the 48 sets of data studied, Table 2 outlines the number of instances in which different surface treatments displayed the features shown in Figure 2. All 27 studied nitrogen doped cavities displayed a prominent dip in the frequency just below the transition. Note that although there exists one instance of a dip in a cavity post nitrogen infusion and one instance of a dip in a cavity post 75/120 C bake, both dips were quite small. As such, this prominent dip in the frequency is concluded to be a signature of N-doped cavities. The effect of different cavity parameters on this dip will now be explored.

Effect of Cavity Design Frequency on the Dip

To study the effect of cavity design frequency on the

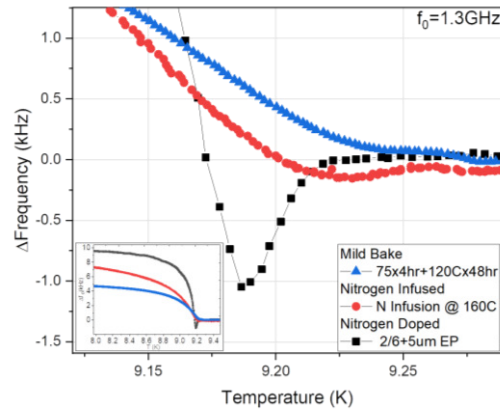


Figure 8: Frequency vs temperature data for a 1.3 GHz single cell cavity subject to three different surface treatments. The inset shows a zoomed-out plot of the three profiles.

Table 2: Occurrences of Features Near T_c Observed for Various Surface Treatments.

	N Doped	N In-fused	75/120 C	120 C	EP
Dip	27	1	1		
Foot		1	4		
Bump			1		1
Dip + Bump		2		1	
Standard		1	4	1	3

dip, four cavities of different resonant frequencies were treated to the same 2/6 nitrogen doping surface treatment. The four resonant frequencies studied were: 650 MHz, 1.3 GHz, 2.6 GHz, and 3.9 GHz. The resulting frequency vs temperature profiles are shown in Figure 9. It is observed that the higher the design frequency of the cavity, the larger the dip. In fact, the figure on the right in Figure 9 shows that the dip depth appears to increase linearly with the design frequency. One simplified possible model to explain this linear relationship could stem from the frequency dependence of the NCing skin depth. Because it goes as the square root of the inverse of frequency, higher resonant frequency cavities will exhibit a shorter skin depth. As such, the discontinuity between the normal conducting skin depth and the penetration depth that occurs at the superconducting transition may increase with frequency, increasing the depth of the observed dip because the skin depth must effectively “catch up” to the penetration depth.

This increase in the magnitude of this dip for higher resonant frequency cavities appears to also have a strong correlation with the frequency dependence of the anti-Q slope of post N-doping, as shown in [11]. Higher resonant

Content from this work may be used under the terms of the CC BY 3.0 licence (© 2019). Any distribution of this work must maintain attribution to the author(s), title of the work, publisher, and DOI.

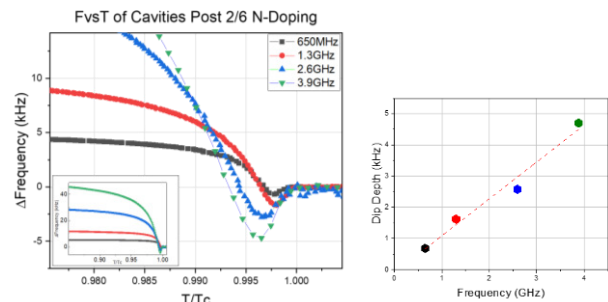


Figure 9: (Left) Frequency vs temperature data for cavities of different resonant frequencies subject to 2/6 N-doping. The lower left inset gives a zoomed-out picture of the FvsT profiles. (Right) Comparison of the dip depth versus the resonant frequency.

frequency cavities exhibit a larger dip depth and stronger anti-Q slope. The relation of these two effects will be the subject of future study.

Effect of Nitrogen Concentration on Dip

To study the effect that nitrogen concentration has on the dip, one single cell 1.3 GHz TESLA shaped Nb SRF cavity, TE1RI003, was treated with the 3/60 nitrogen doping recipe discussed in Table 1. The cavity was then tested after sequential removal of the surface via EP. This sequential removal decreases the concentration of interstitial nitrogen that exists within the RF layer, causing the mean free path (MFP) to increase. The cavity resonant frequency through warm up and the Q_0 vs E_{acc} curves after each step of removal are shown in Figure 10.

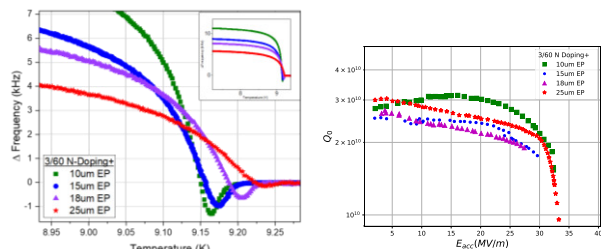


Figure 10: (Left) Effect of nitrogen concentration on the dip in FvsT data for cavity TE1RI003. The inset shows a zoomed-out picture of the profiles. (Right) A plot of Q_0 vs E_{acc} after various amounts of removal all taken at a temperature of 2 K.

After a 10 μm removal of the RF surface, TE1RI003 had a prominent dip in frequency just below T_c . The Q_0 vs E_{acc} curve for this test shows a typical N-doped profile, with the existence of the anti-Q slope phenomenon [1]. After removing an additional 5 μm , giving a total of 15 μm of removal, the dip depth decreased while the transition temperature of the cavity increased. Compared to the previous test, the Q_0 of the cavity was not as high; it also has little to no anti-Q slope. Removing another 3 μm of the surface causes the magnitude of the dip to decrease further and the transition temperature to increase slightly. It should be noted that the Q_0 vs E_{acc} curve of the cavity after a total of 18 μm of removal of the surface showed the onset of high

field Q-slope [12]. However, data was only taken to 27 MV/m to avoid quenching the cavity at 2 K for this test. Further measurements at ~ 1.5 K showed that the cavity reached accelerating gradients up to 36.5 MV/m and was power limited. The final test shown in Figure 10 is after a total removal of 25 μm of the RF surface. The magnitude of the dip is now very small, with a depth of about ~ 100 Hz, which is just above the noise level. In addition, the T_c increases further, up to a value of ~ 9.26 K. In summary, as the concentration of nitrogen decreases, the doping effect gradually diminishes in: 1) the temperature dependence of the penetration depth, 2) the depth of the dip, 3) the Q_0 vs E_{acc} curves.

Some trends with MFP near the surface can be observed from this sequential removal study. The MFP of the cavity after each step of removal was extracted using the BCS Halbritter routine [13]. The MFP values obtained were then plotted against the depth of the dip in frequency, measured relative to the normal conducting value, and against T_c . The results are shown in Figure 11.

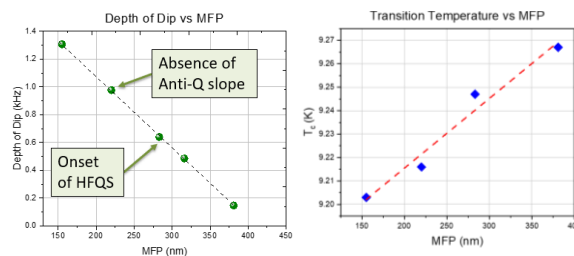


Figure 11: Effect of MFP on (Left) dip depth (Right) transition temperature.

As can be observed above, dip depth appears to vary linearly with the mean free path of the cavity. A mean free path of 220 nm for the cavity corresponds to an absence in the anti-Q slope, as observed in Figure 10 after 15 μm of removal. A mean free path of 283 nm is obtained when the cavity had the onset of high field Q slope. Continuing the linear trend, the dip is expected to disappear entirely when the MFP is ~ 400 nm.

The presence, absence, or magnitude of this dip could give a tool in helping to assess the level of doping in cavities. For undoped EP cavities, the MFP of cavities is very large (>800 nm); as such, from the linear trend observed in Figure 11, a dip is not expected; it is indeed not observed in data. For doped cavities (MFP ~ 100 nm – 300 nm, low BCS that decreases from low to mid-field), a prominent dip is expected. Underdoped cavities, which tend to have higher quench fields and a BCS resistance that is flat or increasing with field, could be defined as the point at which there is no longer an anti-Q slope to the undoped region (~ 220 nm – 400 nm). Heavily-doped cavities (MFP < 100 nm, steep BCS slope, early quench) have not been yet studied but will be the subject of future research.

The transition temperature also appears to have a linear relationship with the mean free path of the cavity. From the plot, it is seen that the effect of nitrogen interstitial on T_c is small, varying only 60 mK for MFP values that range from 150 nm to 380 nm.

DISCUSSION

Origin of Dip

Although this dip in the resonant frequency below the normal conducting value just below the superconducting transition have been discussed elsewhere [14, 15], a short summary of this phenomenon is presented here followed by possible implications. Because the normal conducting skin depth decreases with temperature (due to the longer scattering times of electrons in the Drude model), this skin depth can be pushed into the anomalous regime, making non-local effects important. As a result, Mattis-Bardeen (MB) theory can be used to gain insight on the mechanisms responsible for this dip in the frequency. In MB theory [16], the conductivity of a superconductor is described by

$$\sigma_s = \sigma_1 + i\sigma_2, \quad (2)$$

where σ_1 and σ_2 are conductivities of quasi-particles and Cooper pairs. The surface impedance of the superconductor normalized to the NCing conductivity σ_N is

$$\frac{Z_S}{Z_N} = \left(\frac{\sigma_s}{\sigma_N}\right)^{-1/2}. \quad (3)$$

For there to exist a dip in the frequency below the NCing value, the penetration depth must be longer than the NCing skin depth δ_N . For this to occur, the penetration depth must increase relative to the value of δ_N as the temperature decreases through transition. Using (3), for values where of $(\sigma_s - \sigma_N)/\sigma_N \ll 1$ and if the superconductor is in the dirty limit, Varmazis *et al.* obtain the following expression for the change in the superconducting penetration depth very close to and below T_c :

$$\Delta\lambda = \frac{\delta_N}{4} \left(\frac{\sigma_2}{\sigma_N} - \Delta \left(\frac{\sigma_1}{\sigma_N} \right) \right), \quad (4)$$

where the second term in the parentheses denote a change in the quasi-particle conductivity. This states that for there to exist a dip in the resonant frequency of a cavity close to and below T_c , the increase in the conductivity of the super-electrons must be larger than the increase in the conductivity of the quasi-particles. Thus, the super-electrons in a superconductor are responsible for the existence of a dip in the frequency.

There are two cases that will determine the existence of this dip in a superconductor which involve the mean free path l , the extreme anomalous skin depth $\delta_{N\infty}$, and coherence length ξ_0 :

1. $\delta_{N\infty} < \xi_0$: dip is likely to exist regardless of the value of l
2. $\delta_{N\infty} > \xi_0$: a dip may exist if the mean free path is sufficiently low enough.

In the case of niobium, case 2 is applicable. This means that the mean free path of the cavity will play a role in determining if the phenomenon in question will occur.

This last point is important in helping to understand why only nitrogen doped cavities seem to experience this dip. Electropolished cavities have very long mean free paths (~1000 nm). As such, this fails the case 2 condition laid out above, implying that there should be no dip in the frequency near T_c . Indeed, Table 2 shows that electropolished cavities display only one distinct feature in frequency near T_c in addition to the otherwise expected sharp transition to a plateau in the normal conducting regime. In addition, cavities subject to 120 C bake, 75/120 C bake, and nitrogen infusion tend to have a very short mean free path at the surface; however, this is only true very close to the surface. Further from the surface the MFP becomes very long, failing again the case 2 condition. This, along with the fact that cavities subject to these surface treatments do not display a prominent dip, hints that perhaps the immediate RF surface is not the only region of importance. To contrast this, nitrogen doped cavities have interstitial nitrogen all throughout the RF layer, with mean free paths that are significantly shorter than that of electropolished cavities (~60-400 nm). As a result, cavities subject to this surface treatment are expected to, and do indeed, show a dip in the frequency below the normal conducting value close to and below T_c .

Possible Implications: Differences in Coupling between Electrons and Phonons

In addition to being fundamentally interesting, the dip in the frequency below the normal conducting value near T_c might be indicative of a difference in electron-phonon interactions of SRF cavities. In BCS theory, when plotted against the temperature, there exists a peak in the quasi-particle conductivity, σ_1 [17]. This peak is called the coherence peak and occurs at temperatures of $\sim 0.85T_c$. This coherence peak comes from the increased conductivity of quasi-particles that arises from the breaking of Cooper pairs by thermally activated phonons [18-20]. To couple with the above studies of the effect of nitrogen concentration and frequency on the dip, the effect of the superconducting gap and resonant frequency on the coherence peak are calculated and shown in Figure 12.

Figure 12 shows that the resonant frequency of a cavity strongly controls the height of the coherence peak. Higher frequencies give lower coherence peak heights. Note that the resonant frequency also weakly alters the width, which tends to be centred around ~ 7 K. In contrast, the superconducting gap Δ appears to strongly control the width of the coherence peak, with higher gap values yielding thinner widths of the coherence peak. This coherence peak can be calculated with experimental Q_0 vsT and FvsT data by obtaining first the surface impedance and calculate the conductivity, as discussed in [18]. Such a study was done by [20], where Q_0 vsT and FvsT data were taken on a Nb sample in a 60GHz resonator. The Nb FvsT data shown in this paper presents a dip in the frequency just below T_c , as shown in Figure 13. Note that Klein *et al* report preparing the Nb samples with nitric acid. Using the method laid out in the paper, the Q_0 vsT and FvsT data given there are used to calculate the quasi-particle conductivity. The resulting

quasi-particle conductivity that the authors show is given in Figure 13. The resulting coherence peak was found to be better fit with Eliashberg strong coupling theory, giving first hints that the presence of the dip could be indicative of stronger electron phonon interactions.

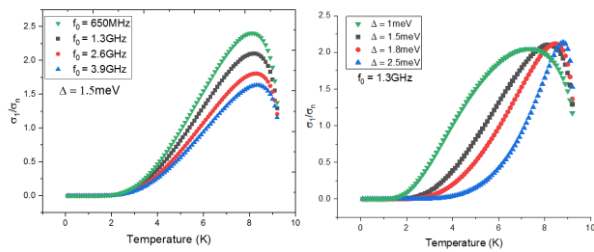


Figure 12: (Left) BCS calculations of the quasi-particle conductivity for various resonant frequencies of cavities with a superconducting gap of 1.5 meV. (Right) BCS calculations of the quasi-particle conductivity for various superconducting gaps for a resonant frequency of 1.3 GHz. Both figures are done for niobium with a T_c of 9.25 K.

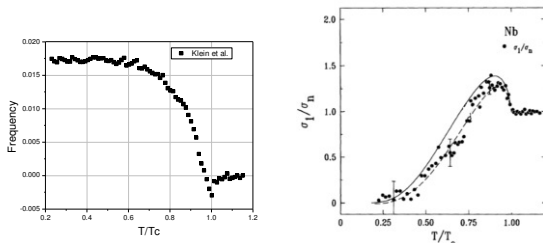


Figure 13: (Left) F vs T data taken from Figure 3 in [20]. (Right) the quasi-particle conductivity as shown in [20]. The solid line gives a BCS weak coupling fit. The dashed line is obtained from Eliashberg strong coupling theory.

One possible cause of this enhanced electron phonon interaction could come from the suppression of the formation of niobium hydrides. Nitrogen interstitial captures hydrogen that exists in the lattice, preventing the nucleation of metallic inclusions that distort the lattice. This could in turn increase electron phonon interaction.

CONCLUSION

Gradients well above 30 MV/m with quality factors up to $6E10$ for nitrogen doped Nb single cell 1.3 GHz SRF cavities have been obtained with optimized surface treatments. TMAP investigations and analysis of the heating profiles of the quench spot suggest that the quench in N-doped cavities could be of magnetic or thermo-magnetic origin.

The depth of the prominent dip in superconducting resonant frequency below the normal conducting value just before the transition temperature of N-doped Nb cavities is shown to increase linearly with the cavity design frequency, showing strong correlation with the frequency dependence of the anti-Q slope of N-doped cavities.

In addition, this dip decreases linearly as the near surface MFP increases, implying that higher concentrations of nitrogen near the RF surface will increase the dip depth. For

a cavity post 3/60 N-doping, the anti-Q slope disappears when the MFP is 220 nm. The onset of HFQS appears when the MFP is 283 nm. This dip is expected to disappear when the MFP ~ 400 nm. In conclusion: as the effect of nitrogen doping on the Q_0 vs E_{acc} curve diminishes, so does its effect on the dip in the frequency. This relationship allows for a quantitative assessment of the level of doping of N-doped cavities that can be used to feed into future models to further understand differences in performance.

The transition temperature of a 1.3 GHz Nb cavity has also been observed to vary with the MFP of nitrogen. The transition temperature increased by 60 mK when the MFP of the 3/60 N-doped cavity TE1RI003 increased from 150 nm to 380 nm, implying that the concentration of nitrogen interstitial has a small but measurable effect on the T_c of cavities.

One possible implication of this dip could be that it signifies an increase in the electron phonon interaction. This could result from the capturing of hydrogen by nitrogen, thereby preventing the formation metallic inclusions in the lattice. To check for differences in electron phonon coupling, the size of the coherence peak that occurs in the quasi-particle conductivity of BCS theory can be used. Future work includes carrying out the calculations presented in Figure 13 on cavities subject to various surface treatments and tested at FNAL.

With this new signature of nitrogen doped cavities, some insight on the microscopic origins of excellent performance has been gained. The full understanding of these mechanisms will help to better tailor surface treatments of Nb SRF cavities that serve as an enabling technology for future accelerators.

REFERENCES

- [1] A. Grassellino *et al.*, *Supercond. Sci. Technol.*, vol. 26, pp. 102001, 2013.
- [2] A. Romanenko, A. Grassellino, A. C. Crawford, D. A. Sergatskov, and O. Melnychuk, *Appl. Phys. Lett.*, vol. 105, 234103, 2014.
- [3] A. Grassellino *et al.*, *Supercond. Sci. Technol.*, vol. 30, pp. 094004, 2017.
- [4] A. Grassellino *et al.*, “Accelerating fields up to 49 MV/m in TESLA-shape superconducting RF niobium cavities via 75C vacuum bake”, 2018. arXiv:1806.09824
- [5] D. Bafia *et al.*, “Low T Bake – Cool Down Studies”, presented TESLA Technology Collaboration Workshop at TRIUMF (TTC’19), Vancouver, Canada, February 5-8, 2019.
- [6] A. Romanenko, A. Grassellino, F. Barkov, and J. P. Ozelis, *Phys. Rev. Spec. Top. Accel. Beams*, vol. 16, pp. 012001, 2013.
- [7] D. Bafia *et al.*, “Quench studies in single cell and multi-cell N-Doped Cavities”, presented TESLA Technology Collaboration Workshop at TRIUMF (TTC’19), Vancouver, Canada, Feb. 5-8, 2019.
- [8] M. Martinello *et al.*, “Magnetic Flux Expulsion in Horizontally Cooled Cavities”, in *Proc. 17th Int. Conf. RF Superconductivity (SRF’15)*, Whistler, Canada, Sep. 2015, paper MOPB014, pp. 110-114.

- Content from this work may be used under the terms of the CC BY 3.0 licence (© 2019). Any distribution of this work must maintain attribution to the author(s), title of the work, publisher, and DOI.
- [9] A. L. Schawlow, G. E. Devlin, *Phys. Rev.*, vol. 113, 1959.
- [10] H. W. Lewis, *Phys. Rev.*, vol. 102, 1956.
- [11] M. Martinello *et al.*, “Field-Enhanced Superconductivity in High-Frequency Niobium Accelerating Cavities,” *Phys. Rev. Lett.*, vol. 121, p. 224801, Nov, 2018. doi: 10.1103/PhysRevLett.121.224801
- [12] A. Romanenko, F. Barkov, L. D. Cooley, A. Grassellino, “Proximity Breakdown of Hydrides in Superconducting Niobium Cavities”, 2013. arXiv: 1212.3384v3
- [13] J. Halbritter, KFK-Extern 3/70–6, 1970.
- [14] C. Varmazis, M. Strongin, *Phys. Rev. B*, vol. 10, 1974.
- [15] C. Varmazis, M. Strongin, *Phys. Rev. B*, vol. 11, 1975.
- [16] D. C. Mattis, J. Bardeen, *Phys. Rev.*, vol. 111, 1958.
- [17] J. Bardeen, L. N. Cooper, J. R. Schrieffer, *Phys. Rev.*, vol. 108, 1957.
- [18] M. R. Trunin, A. A. Zhukov, A. T. Sokolov, *Zh. Eksp., Teor. Fiz.*, vol. 111, pp. 696-704, 1999.
- [19] F. Marsiglio, J. P. Carbotte, R. Akis, D Achkir, M Poirier, *Phys. Rev. B.*, vol. 50, 1994.
- [20] O. Klein, E. J. Nicol, K. Holczer, G. Gruner, *Phys. Rev. B.*, vol. 50, 1994.